

A Sample of Radio Galaxies Spanning Three Decades in Radio Luminosity – The Fundamental Plane & Star Formation Histories

Peter D. Herbert¹*, Matt J. Jarvis¹, Chris J. Willott², Ross J. McLure³, Ewan Mitchell⁴, Steve Rawlings⁴, Gary J. Hill⁵, James S. Dunlop³

¹Centre for Astrophysics Research, Science & Technology Research Institute, University of Hertfordshire, Hatfield, AL10 9AB, UK

²Herzberg Institute of Astrophysics, National Research Council, 5071 West Saanich Road, Victoria, BC V9E 2E7, Canada

³SUPA Institute for Astronomy, University of Edinburgh, Royal Observatory, Edinburgh, EH9 3HJ, UK

⁴University of Oxford, Astrophysics, Department of Physics, Keble Road, Oxford, OX1 3RH, UK

⁵McDonald Observatory, University of Texas at Austin, 1 University Station C1402, Austin, TX 78712-1083, USA

* Email : p.d.herbert@herts.ac.uk

We present the results of our complete investigation of the host galaxies and environments of a sample of radio galaxies spanning a factor of 1000 in radio luminosity at a single cosmic epoch ($0.4 < z < 0.6$). We describe our investigations into the Fundamental Plane of $z \sim 0.5$ radio galaxies using deep spectroscopic data

combined with the HST data from McLure et al. (2004). We find evidence for a $z \sim 0.5$ Fundamental Plane that is somewhat different to that observed in the local universe and discuss possible reasons for this discrepancy. We also find evidence of different star formation histories for high- and low-luminosity radio galaxies.

The Sample

Our 41 object $z \approx 0.5$ radio-galaxy sample consists of all of the narrow-line radio galaxies in the redshift interval $0.4 < z < 0.6$ from four complete, low-frequency selected radio surveys: 3CRR, 6CE, 7CRS and TexOx-1000 (“TOOT”). Full details of the sample (including motivations for this choice of sample) can be found in McLure et al. (2004), along with HST *I*-band imaging data and 2-dimensional modelling of the host galaxies, the results of which we use below.

The Fundamental Plane

We use deep spectroscopic data (from the WHT and Gemini) together with a direct fitting code to obtain the stellar velocity dispersions of 24 of the objects in our sample (Figure 1). We apply an aperture correction using the procedure described by Jørgensen, Franx & Kjørgaard (1995) and combine these results with the effective radii (r_e) and surface brightnesses (I_e) from McLure et al. (2004). We show in Figure 2 the location of our objects on the Fundamental Plane of local active galaxies (Bettoni et al. 2001). The majority of the radio galaxies in the sample of Bettoni et al. (2001) are FRIs. We then fit a plane to our data by minimising the sum of the squared residuals perpendicular to the plane, weighted by the errors on the residuals. We show our best fitting plane in Figure 3.

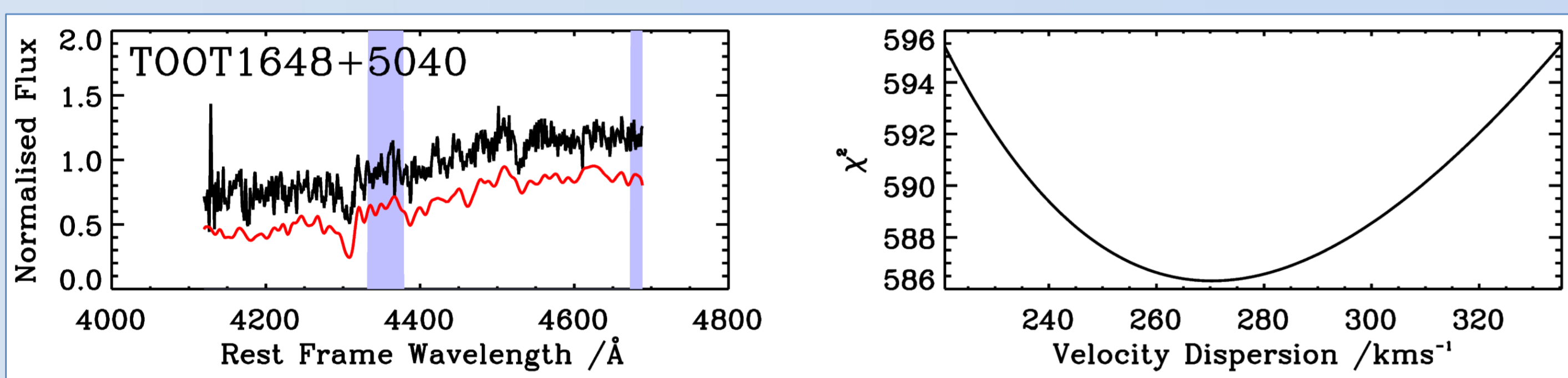


Figure 1. Left panel: the TOOT1648+5040 spectrum (black) overlaid with our best fitting broadened template (red; offset by 0.3) and with shaded regions excluded from the fit due to emission or absorption features. Right panel: the minimisation of χ^2 as a function of σ .

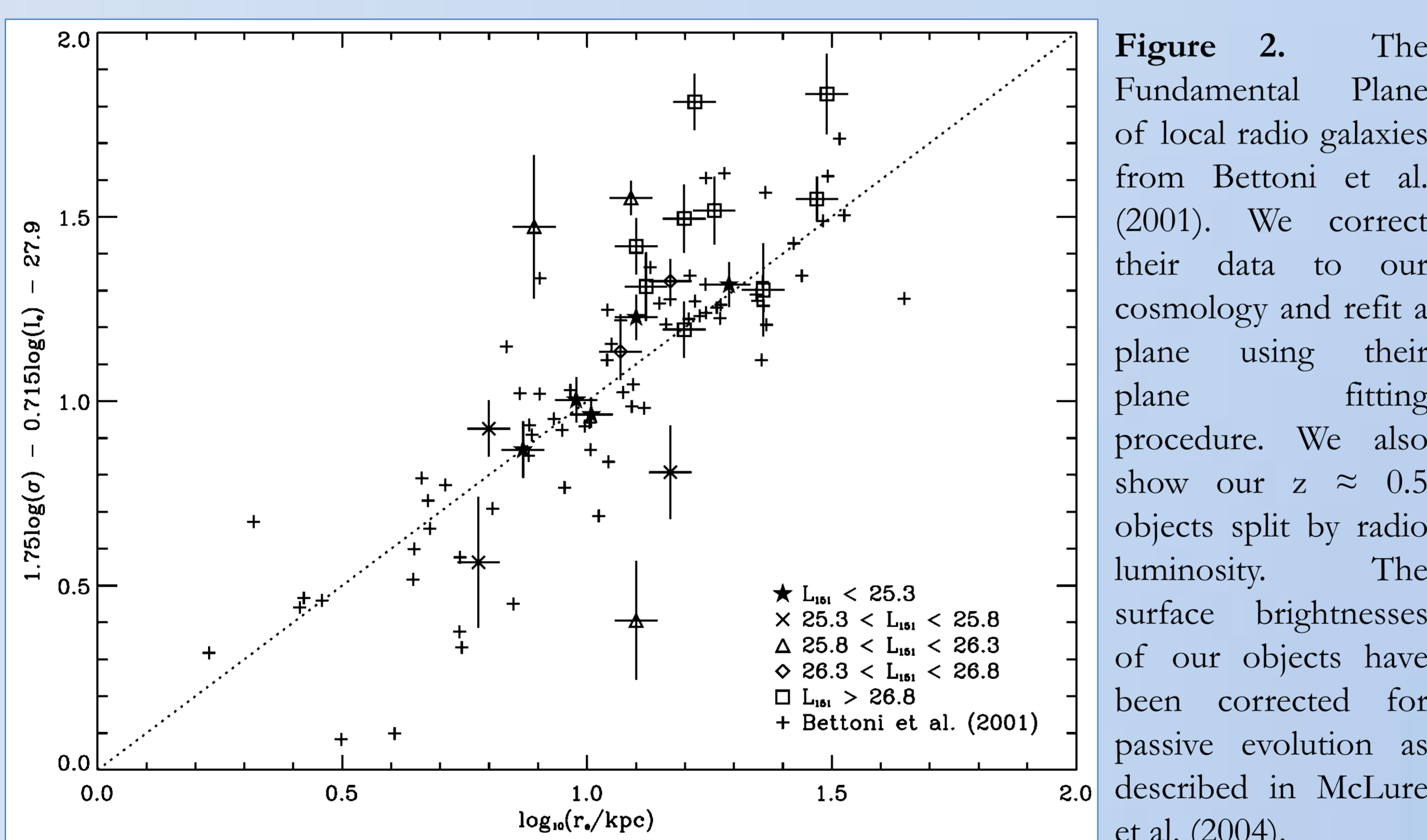


Figure 2. The Fundamental Plane of local radio galaxies from Bettoni et al. (2001). We correct their data to our cosmology and refit a plane using their fitting procedure. We also show our $z \approx 0.5$ objects split by radio luminosity. The surface brightnesses of our objects have been corrected for passive evolution as described in McLure et al. (2004).

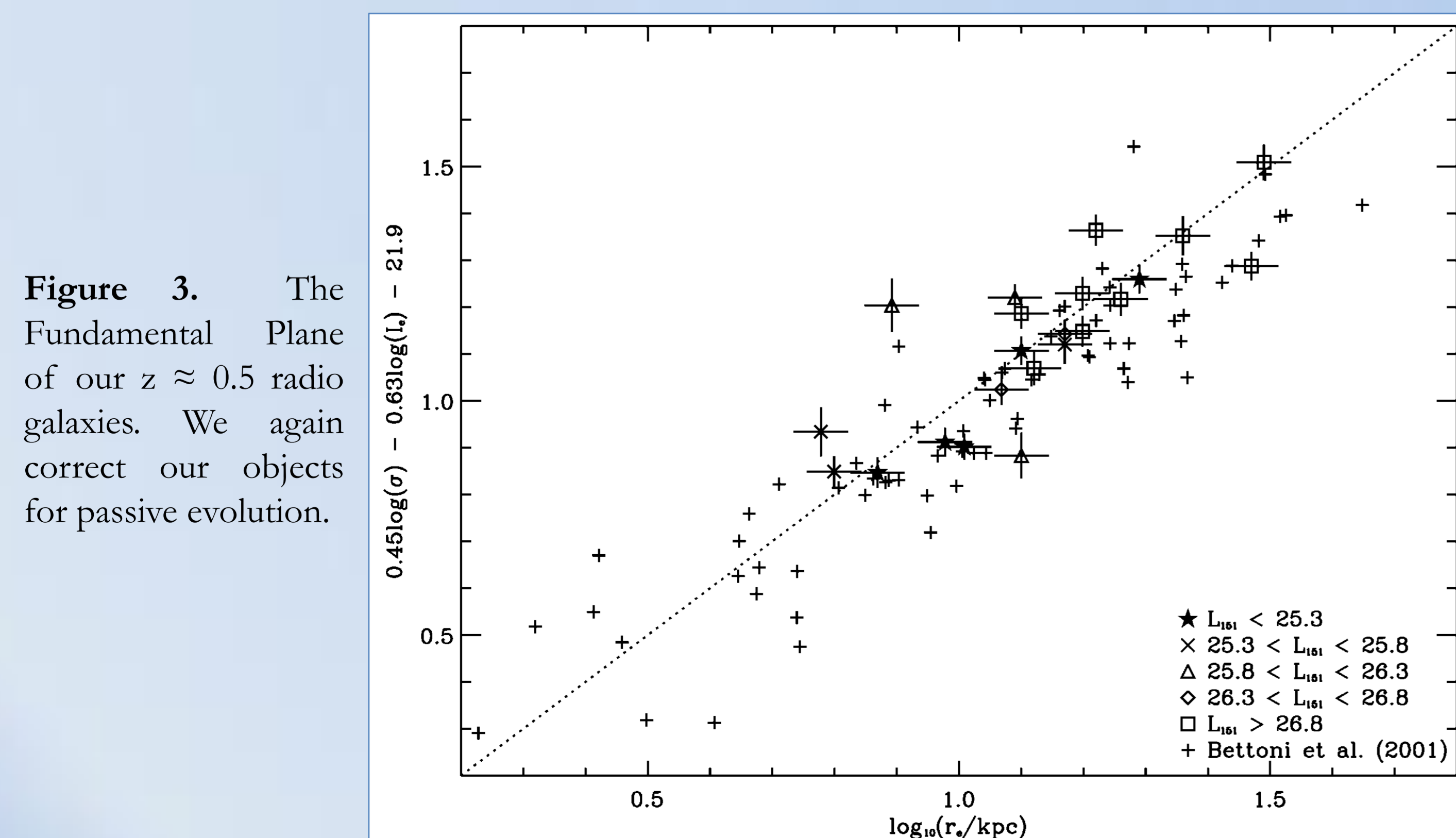


Figure 3. The Fundamental Plane of our $z \approx 0.5$ radio galaxies. We again correct our objects for passive evolution.

We find that our lower-luminosity objects ($L_{151} < 10^{25.3} \text{ W Hz}^{-1} \text{ sr}^{-1}$; FRIs) fall on the local relation but objects with higher radio luminosities (FRIs) typically do not. In Herbert et al. (in prep) we consider two possible explanations:

1. **The Fundamental Plane is different for low- & high-luminosity radio galaxies.**
2. **Evolution of the host galaxies.** In Herbert et al. (in prep) we examine whether passive evolution, a mass-dependent change in the mass-to-light ratio, or size evolution can explain the difference between the planes. We find that none of these can in isolation provide the solution, but suggest that some combination of all three may provide a plausible explanation.

Star Formation Histories

We use the strength of the 4000Å break (the $D_n(4000)$ index) as an indicator of recent star formation; younger stellar populations have smaller 4000Å breaks (see Herbert et al. 2010 for full details). In Figure 4 we show $D_n(4000)$ versus the low-frequency radio luminosity at 151 MHz, L_{151} , for our objects. We find:

1. Evidence of different star formation histories for high- (typically FRII) and low-luminosity (typically FRI) radio sources.
2. The sample is also fairly well divided by the spectral classification scheme of Hine & Longair (1979): low excitation galaxies (LEGs) possess older stellar populations than high excitation line objects (HEGs).

These results are consistent with the hypothesis that HEGs are powered by accretion of cold gas, which could be supplied, for example, by recent mergers, secular instabilities, or filamentary cold flows. These could also trigger star formation in the host galaxy. The LEGs do not show evidence for recent star formation and an influx of cold gas, and are consistent with being powered by the accretion of the hot phase of the inter-stellar medium (Hardcastle, Evans & Croston 2007, 2009).

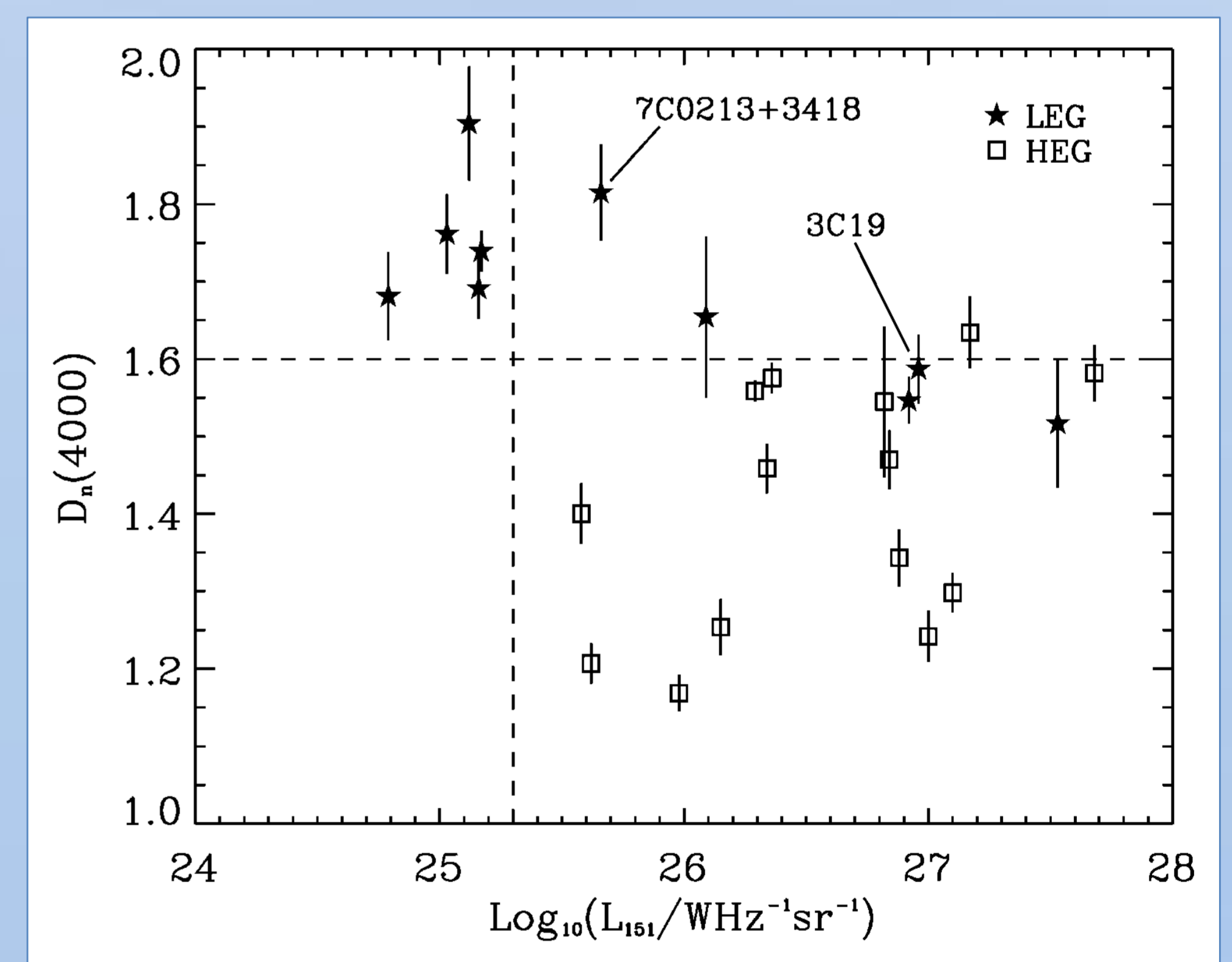


Figure 4. $D_n(4000)$ versus L_{151} , split by spectral classification (Hine & Longair 1979).

Future Work: The Cluster Environments

We have recently completed wide field imaging in the g, r and i bands of all of our sample using the Isaac Newton Telescope (see Figure 5). We are currently engaged in using multi-colour images to investigate the cluster environments of our radio galaxies to determine whether the environmental density is related to the central radio galaxy, and whether there is a preferred orientation for the radio jets with respect to the environment.

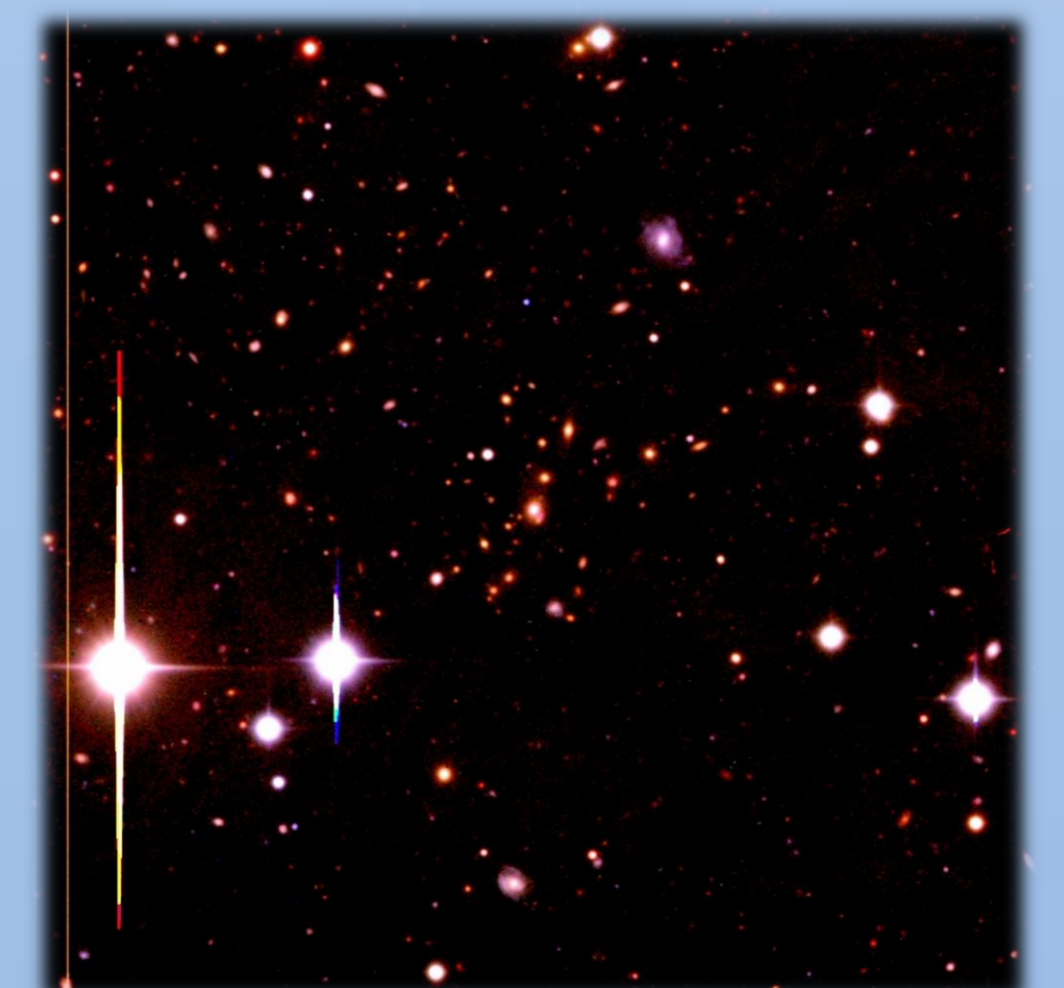


Figure 5. Multi-colour image of the 5×5 arcmin² field around 3C244.1.

References

- Bettoni, D. et al., 2001, A&A, 380, 471
 Hardcastle M.J., Evans D.A. & Croston J.H., 2007, MNRAS, 376, 1849
 Hardcastle M.J., Evans D.A. & Croston J.H., 2009, MNRAS, 396, 1929
 Herbert, P.D. et al., 2010, MNRAS, in press (arXiv:1004.1099)
 Hine R.G. & Longair M.S., 1979, MNRAS, 188, 111
 Jørgensen I., Franx M. & Kjørgaard P., 1995, MNRAS, 276, 1341
 McLure R.J. et al., 2004, MNRAS, 351, 347